

# The electrochemical phase behaviour of chemically asymmetric lipid bilayers supported at Au(111) electrodes

Madrid, Elena; Horswell, Sarah L

DOI:

[10.1016/j.jelechem.2017.11.006](https://doi.org/10.1016/j.jelechem.2017.11.006)

License:

Creative Commons: Attribution-NonCommercial-NoDerivs (CC BY-NC-ND)

*Document Version*

Peer reviewed version

*Citation for published version (Harvard):*

Madrid, E & Horswell, SL 2017, 'The electrochemical phase behaviour of chemically asymmetric lipid bilayers supported at Au(111) electrodes', *Journal of Electroanalytical Chemistry*, pp. 338-346.

<https://doi.org/10.1016/j.jelechem.2017.11.006>

[Link to publication on Research at Birmingham portal](#)

## General rights

Unless a licence is specified above, all rights (including copyright and moral rights) in this document are retained by the authors and/or the copyright holders. The express permission of the copyright holder must be obtained for any use of this material other than for purposes permitted by law.

- Users may freely distribute the URL that is used to identify this publication.
- Users may download and/or print one copy of the publication from the University of Birmingham research portal for the purpose of private study or non-commercial research.
- User may use extracts from the document in line with the concept of 'fair dealing' under the Copyright, Designs and Patents Act 1988 (?)
- Users may not further distribute the material nor use it for the purposes of commercial gain.

Where a licence is displayed above, please note the terms and conditions of the licence govern your use of this document.

When citing, please reference the published version.

## Take down policy

While the University of Birmingham exercises care and attention in making items available there are rare occasions when an item has been uploaded in error or has been deemed to be commercially or otherwise sensitive.

If you believe that this is the case for this document, please contact [UBIRA@lists.bham.ac.uk](mailto:UBIRA@lists.bham.ac.uk) providing details and we will remove access to the work immediately and investigate.

# ***The Electrochemical Phase Behaviour of Chemically Asymmetric Lipid Bilayers Supported at Au(111) Electrodes***

Elena Madrid<sup>1</sup> and Sarah L. Horswell\*

*School of Chemistry, University of Birmingham, Edgbaston, Birmingham B15 2TT, United Kingdom*

<sup>1</sup> Present address: *Department of Chemistry, University of Bath, Claverton Down, Bath BA2 7ZA, UK*

\* s.l.horswell@bham.ac.uk

## **Abstract**

Chemically asymmetric phospholipid bilayers supported on Au(111) surfaces have been studied with differential capacitance and chronocoulometry measurements. The bilayers were prepared using Langmuir-Blodgett deposition, followed by Langmuir-Schaeffer deposition using a different molecule. Combinations of three phospholipids with common hydrocarbon tail groups were compared: dimyristoyl phosphatidyl choline (DMPC), dimyristoyl phosphatidyl ethanolamine (DMPE) and dimyristoyl phosphatidyl serine (DMPS). DMPC and DMPE are zwitterionic and DMPS is anionic in the electrolyte used. The asymmetric bilayers containing DMPS gave distinct electrochemical responses depending on whether the DMPS was deposited first, onto Au, or second, onto another lipid, indicating that asymmetry was maintained over the timescale of the experiment. The results for DMPE and DMPC combinations suggest similar headgroup conformations in the two bilayers. The relationship between the location of the charged molecule and the electrochemical properties is complex but in all cases, DMPS tends to raise bilayer capacitance and DMPE tends to lower capacitance. These observations can be explained by the relatively higher solvation of the charged DMPS molecules and tight packing of DMPE molecules, which leads to exclusion of solvent from the bilayer.

## **Keywords**

phospholipid

asymmetric bilayer

adsorption

electrochemistry

capacitance

*N.B.* Print version to include figures as black and white.

## 1. Introduction

The basis of a biological cell membrane is a bilayer of lipids, which assemble to form a selective barrier between the two aqueous environments on either side [1]. The lipids are amphiphiles; that is, they have a hydrophilic (polar) headgroup and hydrophobic tail groups. Consequently, when dispersed in water they tend to assemble in such a way as to keep the polar headgroups in contact with the aqueous phases and the hydrophobic chains in proximity with each other but away from water. In the cell membrane, a bilayer is formed in which the hydrophobic chains of each monolayer face one another in the interior and the headgroups face the aqueous environment on either side of the membrane. Embedded in this bilayer are various proteins, each of which has a particular function, for example to act as a receptor or to control passage of ions or small molecules in and out of the cell (or compartment within a cell) [1]. Some of these proteins have specific interactions with certain lipids [1–3] and so it is of interest to understand the behaviour of a range of lipids within a membrane.

Many mimics of these membranes have been studied, including vesicles, black lipid membranes, lipid monolayers on water, supported lipid monolayers and supported lipid bilayers. In the last two cases, the support can be a metal, which affords the possibility to study the effect of an applied electric field on the lipid layer [4,5]. This is of interest because natural cell membranes often experience fields of up to  $10^7$ – $10^8$  V m<sup>-1</sup> that result from charge asymmetry and/or ion gradients across the membrane [4–7]. Monolayer studies have mainly been made with mercury electrodes, in which a mercury drop is pushed through a monolayer of the lipids on an aqueous subphase [8–25]. Mercury's smooth surface allows the formation of practically defect-free monolayers (indicated by very low capacitance). These monolayers normally have the tail groups facing the hydrophobic mercury and the headgroups facing the water, although it is possible to invert the monolayer by applying a very strong electric field [10]. Studies have included investigating this phase behaviour with differential capacitance, coulometry, ion reduction and electrochemical impedance spectroscopy [9–14], as well as determining the surface dipole and surface charge density of the monolayers [8, 15–17]. Further publications have explored the redox mechanism of ubiquinone contained within the layers [18, 19] and interactions of the monolayers with ion-forming proteins [20–22]. Proteins have also been studied in tethered lipid layers [23, 24]. Solid-supported lipid bilayers have also been studied and these investigations have tended to focus on the structural changes occurring within the bilayers as the applied field is varied, exploiting the possibility of using surface science techniques *in situ* [4]. By using a range of these probes: vibrational spectroscopy [4,5,7, 26–30], scanning probe microscopy [31, 32] and reflectometry [6, 33], a detailed picture can be built up at the molecular level to describe how the lipid bilayer responds to the electric field [4]. In addition, the insertion of proteins into the bilayers (or into tethered bilayers on surfaces) can be studied [34–37].

Most of these studies have used symmetric bilayers as mimics of the membrane, although selective deuteration has been employed to study each monolayer separately [26, 29] and, in some cases, specific molecules have been included in the electrolyte-facing layer to study their behaviour [30]. However, real membranes are often asymmetric: the composition of each monolayer is different. In a mammalian plasma cell membrane, the outer monolayer is rich in phosphatidyl cholines (PC) and sphingomyelin (SM) (Figure 1) and the inner monolayer contains more phosphatidyl ethanolamine (PE) and phosphatidyl serine (PS), which have smaller headgroups [1]. This asymmetry is important

for the cell's function; for example, the aforementioned specific interactions with proteins, and the fact that apoptosis results when PS is exposed on the outer side of the cell. There has been some controversy over the rate of exchange of lipids between the two monolayers: traditionally, lipids were believed to be mobile within a monolayer but to traverse the membrane at a much slower rate, with the movement of lipids between the two leaflets of the bilayer controlled by enzymes known as scramblases and flippases [1]. On the other hand, several sum frequency generation studies [38–41] have shown that the rate of "flip-flop" in some lipid systems is much higher than originally thought, of the order of  $2 \times 10^{-3} \text{ s}^{-1}$  for dimyristoyl phosphatidyl choline (DMPC) at  $5^\circ\text{C}$  below its phase transition, for example [39]. In the present study, we explore the electrochemical phase behaviour of a series of asymmetric bilayers, to determine whether asymmetry is maintained and whether it has an effect on electrochemical properties of the bilayers. We focus on three phospholipid molecules for which the phase behaviour of their symmetric bilayers has been reported: dimyristoyl phosphatidyl choline (DMPC), dimyristoyl phosphatidyl ethanolamine (DMPE) and dimyristoyl phosphatidyl serine (DMPS). These lipids have the same hydrocarbon chains but different headgroups and the difference in headgroups has been shown to affect packing of molecules and, consequently, their electrochemical barrier properties [27,28]. DMPE is particularly well-packed, which will reduce the rate of exchange of lipids between the two halves of the bilayer. (Previous PM-IRRAS results also indicate that selectively deuterated DMPC layers seemed to retain asymmetry [26].) Of particular interest is the effect of the anionic charge on the DMPS molecule and whether its location on the metal-facing monolayer or electrolyte-facing monolayer affects phase behaviour. Although real cell membranes may contain only between 10% and 50% anionic lipids, for simplicity we start by making bilayers which are composed of (nominally) single-component monolayers. We show that the electrochemical responses of these chemically asymmetric bilayers differ from one another and from those of symmetric bilayers, which demonstrates that it is feasible to study asymmetric systems on these timescales. Similar effects of molecule structure are seen to the previously published symmetric systems, in that DMPE tends to lower bilayer capacitance and DMPS seems to raise it. The location of the anionic lipid (in the Au-facing or electrolyte-facing monolayer) affects electrochemical response in a complex way, which has implications for the design of model bilayers in which charge asymmetry is important for protein function.

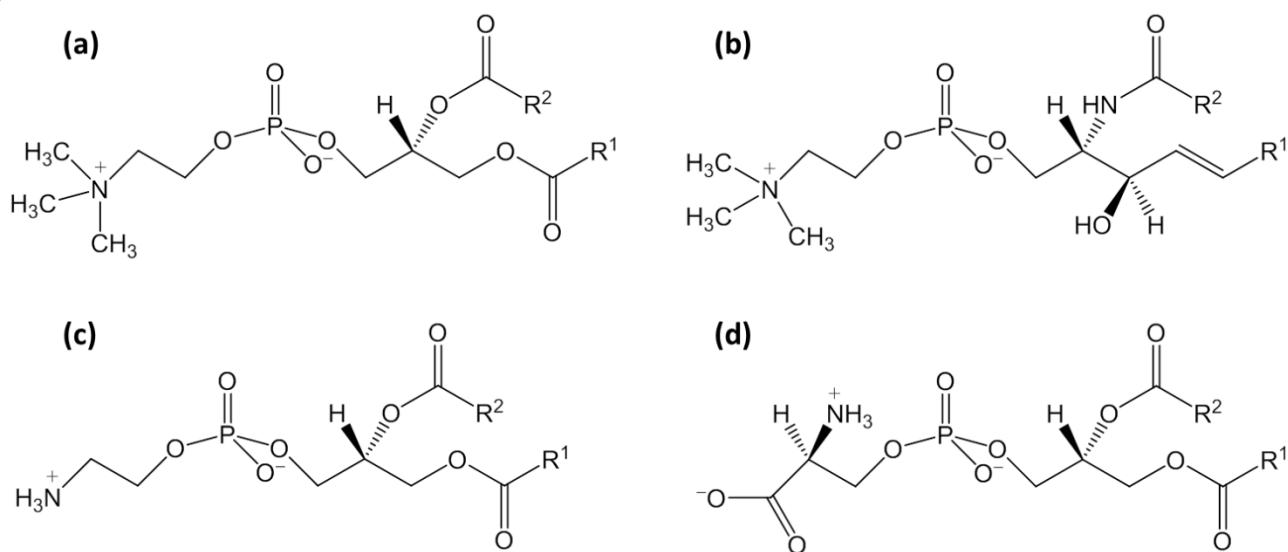


**Figure 1** Structures of common lipids found in mammalian cell membranes. (a) phosphatidyl choline (PC), (b) sphingomyelin (SM), (c) phosphatidylethanolamine (PE), (d) phosphatidylserine (PS).

## 2. Experimental

### 2.1 Materials and cleaning

Water purified with a Milli-Q gradient A10 system was used throughout, for all cleaning and solutions. Electrolyte solutions were prepared from sodium fluoride (99.99%, Alfa Aesar) and ultrapure water. All lipids were purchased from Avanti Polar Lipids Inc. (AL, USA) and used without further purification. Methanol and chloroform were HPLC grade and obtained from Sigma Aldrich. Lipid solutions were made up in a mixture comprising 10% methanol and 90% chloroform.

Volumetric flasks were cleaned with piranha solution (*caution – this mixture can cause explosion*), followed by rinsing thoroughly with ultrapure water and soaking overnight in ultrapure water. Those flasks used for the preparation of lipid solutions were rinsed several times with methanol, then methanol/chloroform solution, to remove water before making up the lipid solution. Other glassware was cleaned by heating for 1 h in a 50:50 mixture of nitric and sulphuric acids, followed by cooling, rinsing with copious amounts of ultrapure water and soaking overnight in ultrapure water.

### 2.2 Bilayer preparation

Lipid bilayers were prepared on Au(111) substrates using a Langmuir-Blodgett (LB) deposition followed by a Langmuir-Schaeffer (LS) deposition. This process enabled asymmetric bilayers to be produced when the lipid deposited in the LS step was different from that deposited in the LB step. The Langmuir trough (Nima, Coventry, UK) was cleaned with chloroform/methanol, then with chloroform, before being filled with ultrapure water. The trough was fitted with a Delrin barrier and a paper Wilhelmy plate. The cleanliness of the water phase was checked before the Au sample was placed in the trough, by closing the barrier and checking the surface pressure remained at zero. The Au(111) substrate was flame-annealed as described previously [42] and transferred with a drop of ultrapure water into the trough. It was lowered into the water sub-phase and the cleanliness of the sub-phase confirmed. A sufficient quantity of lipid solution (typically  $\sim 50 \mu\text{L}$  of a  $1 \text{ mg mL}^{-1}$  solution) was placed onto the surface of the water using a microlitre syringe and left to equilibrate for *ca* 30 min. The barrier was closed at a speed of  $25 \text{ cm}^2 \text{ min}^{-1}$  (total trough area  $600 \text{ cm}^2$ ) to a target pressure of  $40 \text{ mN m}^{-1}$  for DMPC (area per molecule  $45.6 \text{ \AA}^2$ ) or  $47 \text{ mN m}^{-1}$  for DMPE or DMPS (area per molecule  $35\text{--}36 \text{ \AA}^2$ ). At these target pressures, the lipids were in the same phase as for bilayers produced in previous publications[26–29]: the DMPC was in the liquid condensed phase and the DMPE and DMPS were in the solid phase. The sample was raised through the air|water interface at a speed of  $2 \text{ mm min}^{-1}$ , with the pressure maintained at the target pressure, and then dried in argon for 30 min. The lipid monolayer was removed from the water surface and replaced with a monolayer of the other lipid, which was compressed to the appropriate target pressure. A Langmuir-Schaeffer (horizontal dip) was then performed at a speed of  $2 \text{ mm min}^{-1}$ . Depositions were carried out at  $19^\circ\text{C}$ . The sample was placed immediately into an argon atmosphere in the electrochemical cell.

### 2.3 Electrochemical measurements

A glass three-electrode cell was employed for electrochemical measurements. The working electrode was a Au(111) single crystal oriented to better than  $0.5^\circ$  (Mateck, Germany). The counter electrode was a gold coil (99.995%, Alfa Aesar) and the reference electrode was a saturated calomel electrode (SCE). This electrode was housed in saturated KCl solution and connected to the cell *via* a salt bridge. Since previous publications have reported data with respect to a Ag|AgCl|3 M KCl electrode, all potentials reported herein are quoted with respect to that reference electrode, to facilitate comparison. The electrolyte was 0.1 M sodium fluoride and was de-oxygenated before measurements by bubbling with argon. An argon atmosphere was maintained above the solution throughout the measurements.

The potentiostat was a Heka PG590 and was connected to a computer *via* a BNC block and data acquisition board (M series, National Instruments). The computer was used to record data and also to control the waveform of the chronocoulometry measurements, with software kindly provided by Dr Alexei Pinheiro (Universidade Tecnológica Federal do Parana, Londrina, Brazil). For differential capacity measurements, a DSP 7265 dual channel lock-in amplifier (Ametek, Germany) was coupled with the potentiostat to superimpose a 5 mV sinusoidal waveform of frequency 20 Hz onto a  $5 \text{ mV s}^{-1}$  potential sweep. The lock-in amplifier resolved the resulting a.c. response into the in-phase and quadrature components with respect to the applied voltage signal. These components were then used to calculate the capacitance, assuming a series RC circuit.

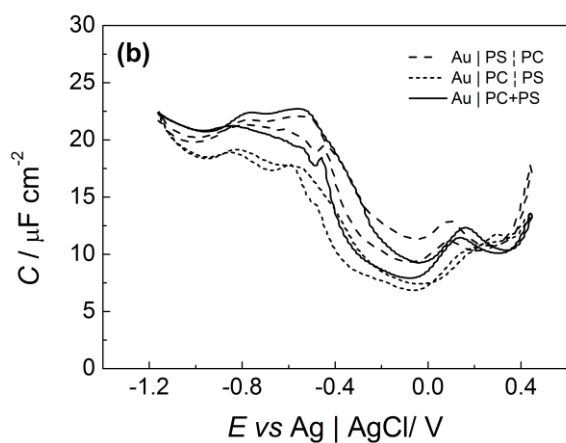
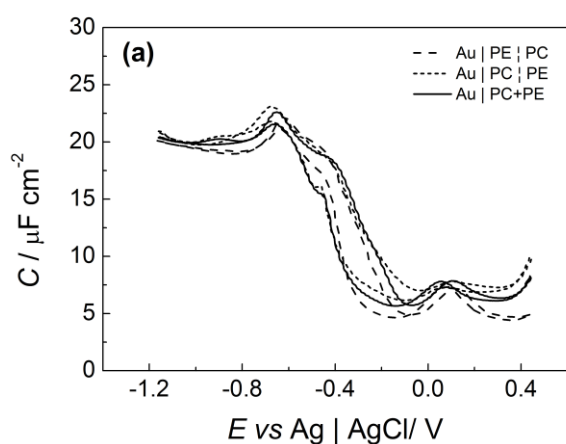
Chronocoulometry experiments were carried out with the same waveform as described previously [27–29]. The potential was held at the potential of interest for 3 min and then stepped briefly to the desorption potential (determined from the differential capacity curves) before being held at a base potential ( $-0.06 \text{ V}$ ) for 1 min. The potential was then stepped to the next potential of interest and the process repeated for all potentials, at intervals of 50 mV. The current transient on the desorption step was integrated to provide the difference in charge densities between the potential of interest and the desorption potential (the relative charge density). Since the potential of zero charge (pzc) of the uncoated Au(111) sample in the base electrolyte is 0.315 V, the charge density-potential curve can then be shifted such that the charge density at this potential is zero [42]. The charge density of the Au(111) surface with lipids should be equal to that measured in the absence of lipids at the potentials where desorption occurs; therefore, the plot of relative charge density can be shifted to match that of the base electrolyte at these potentials to yield a plot of absolute charge density *vs* potential.

## 3. Results and Discussion

### 3.1 Differential Capacitance measurements

Figure 2a presents comparisons of the differential capacitance curves acquired for Au | DMPC | DMPE, Au | DMPE | DMPC and for nominally mixed symmetric bilayers of DMPE and DMPC in a 1:1 ratio (denoted Au | PC+PE). Figure 2b presents similar data for bilayers containing DMPC and DMPS; Figure 2c presents the corresponding results for bilayers containing DMPE and DMPS. The essential features of the capacitance curves are similar to those observed previously for symmetric bilayers of phospholipids [6,27,28]. In the more positive potential region, where charge densities are low, the capacity is lower than that in the absence of lipids, which

indicates that the molecules are adsorbed on the surface. The outer Helmholtz plane is separated farther from the electrode surface by the lipid molecules; this fact, combined with the lower average permittivity of the hydrocarbon chain region than of interfacial electrolyte, causes a drop in capacity. As the potential is made more negative, a phase transition occurs, indicated by the rise in capacity. Neutron reflectivity studies have indicated (for DMPC/cholesterol bilayers) that the lipids are separated from the Au surface by a water cushion, in this potential range, whereas at positive potentials they are directly adsorbed on the surface [6]. At the negative potential limit, the lipid molecules are desorbed and the capacity curves merge with that of the base electrolyte [6]. The hysteresis between the positive-going and negative-going sweeps indicates kinetics may play a rôle in the adsorption and desorption processes.



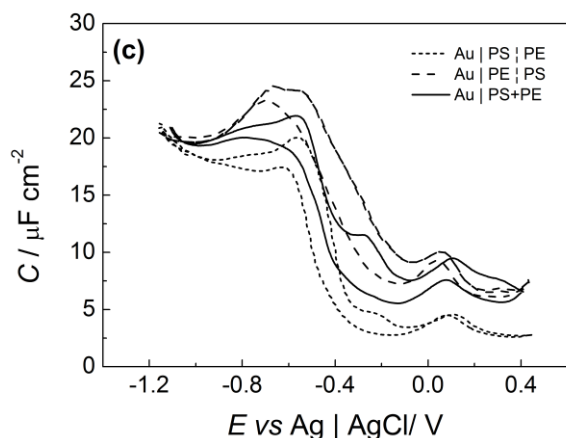


**Figure 2** Differential capacitance vs potential plots for bilayers of different compositions, measured in 0.1 M NaF. (a) Dotted line Au | DMPC | DMPE, dashed line Au | DMPE | DMPC, solid line Au | PC+PE (where both monolayers contain 1:1 DMPE and DMPC). (b) Dotted line Au | DMPC | DMPS, dashed line Au | DMPS | DMPC PCPS, solid line Au | PC+PS (where both monolayers contain 1:1 DMPS and DMPC). (c) Dotted line Au | DMPS | DMPE, dashed line Au | DMPE | DMPS, solid line Au | PS+PE (where both monolayers contain 1:1 DMPE and DMPS).

The biggest differences in differential capacity results are observed for the combination of DMPE and DMPS: the capacity of the Au | DMPS | DMPE film in the positive potential region is clearly lower than that of the mixed bilayer, which is in turn lower than that of the Au | DMPE | DMPS film. The potential of the phase transition is also slightly shifted for the bilayer where DMPS faces the electrolyte. The differences in electrochemical response between the bilayers containing DMPC and DMPS are relatively minor. The differential capacitance curves are similar in shape but the capacity at positive potentials (low charge density) shows the opposite tendency to bilayers containing DMPE and DMPS: the Au | DMPC | DMPS bilayer has lower capacity than Au | DMPS | DMPC. Both DMPC and DMPS are likely to contain more solvent than DMPE [27,28]. The presence of solvent in the bilayer raises the average permittivity of the hydrocarbon chain region, which gives rise to higher values of capacitance. It is possible that the presence of solvent in both halves of the bilayer leads to similar values of capacitance, whereas when DMPE forms one half of the film, the capacitance is lower. The main difference between the curves obtained for DMPC and DMPE bilayers is the shape of the plot at positive potentials: the slightly sloped plot for Au | DMPC | DMPE resembles that observed for Au | DMPC | DMPC and the level plot for Au | DMPE | DMPC resembles that observed for Au | DMPE | DMPE. The mixed bilayer has behaviour in between those of the asymmetric layers. At first sight it appears that the electrical properties are more strongly dependent on the first monolayer deposited than the second.

The coverage of the Au(111) surface can be estimated from Eqn 1 [43]:

$$\theta = \frac{C_0 - C}{C_0 - C_1} \quad \text{Eqn 1}$$



where  $C$  is the measured capacity of the electrode coated in the bilayer,  $C_0$  is the capacity of the bare electrode surface and  $C_1$  is the capacity of the electrode coated in a defect-free bilayer. The capacity of a phospholipid monolayer on Hg is  $\sim 1.6 \mu\text{F cm}^{-2}$  [8], so a value of  $0.8 \mu\text{F cm}^{-2}$  can be expected for a bilayer with few or no defects. Typically, values have been reported at *ca* 0.2 V *vs* SCE, where  $C_0$  is around  $35 \mu\text{F cm}^{-2}$ . We compare coverages estimated from our differential capacity curves in Table 1. We also include values measured at -0.1 V and at -0.2 V because some bilayers exhibit a minimum in capacity at these potentials. It is useful to compare the results with a common layer facing gold and the results with a common layer facing the electrolyte. Comparative plots are presented in Figure 3, which also include data for symmetric bilayers. Looking first at where DMPC is on the Au, the adsorption/desorption and phase transitions for the three bilayers are similar. Capacity and hence coverage values are similar at -0.1 V and at -0.2 V but at 0.2 V, the DMPC system decreases in coverage. This may be a result of an onset of desorption, which is prevented to some extent by a tightly packed DMPE monolayer in Au | DMPC | DMPE, or it may be a result of reorientation of water within the film (DMPE contains less water than DMPC and DMPS). When DMPC faces the solution, again the lowest capacity is observed when DMPE forms part of the bilayer.

**Table 1** Values of % coverage estimated from differential capacitance curves.<sup>a</sup>

Bilayer / Potential	+0.2 V	-0.1 V	-0.2 V
Au   PC   PC	53	74	77
Au   PE   PE	97	88	92
Au   PS   PS	71	42	52
Au   PC   PE	73	76	78
Au   PE   PC	89	82	85
Au   PC+PE	83	78	78
Au   PC   PS	73	73	73
Au   PS   PC	73	62	64
Au   PC+PS	72	68	71
Au   PE   PS	85	69	73
Au   PS   PE	94	90	92
Au   PE+PS	84	79	79

<sup>a</sup>For comparison, the reported capacitance for DMPC bilayers on Au [26] leads to a value of  $\sim 86\%$ . Values for DMPE bilayers taken from data in ref. [27] and for DMPS from data in ref. [28]. The estimated error in the coverage values is 10%.

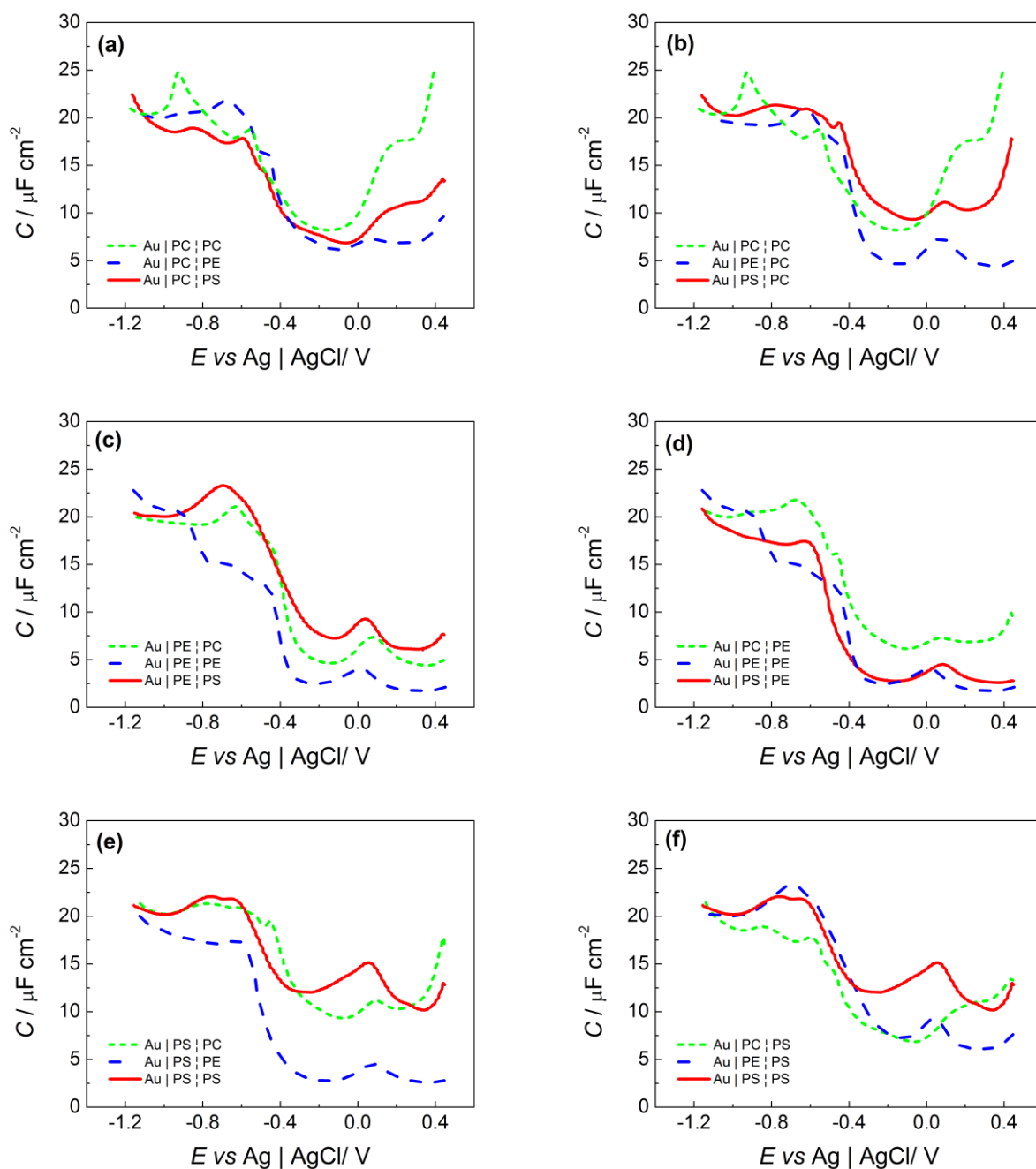


**Figure 3** Differential capacitance vs potential plots (cathodic sweep), in 0.1 M NaF, comparing bilayers with a common layer. (a) Dotted green line Au | DMPC | DMPC, dashed blue line Au | DMPC | DMPE, solid red line Au | DMPC | DMPS. (b) Dotted green line Au | DMPC | DMPC, dashed blue line Au | DMPE | DMPC, solid red line Au | DMPS | DMPC. (c) Dotted green line Au | DMPE | DMPC, dashed blue line Au | DMPE | DMPE, solid red line Au | DMPE | DMPS. (d) Dotted green line Au | DMPC | DMPE, dashed blue line Au | DMPE | DMPE, solid red line Au | DMPS | DMPE. (e) Dotted green line Au | DMPS | DMPC, dashed blue line Au | DMPS | DMPE, solid red line Au | DMPS | DMPS. (f) Dotted green line Au | DMPC | DMPS, dashed blue line Au | DMPE | DMPS, solid red line Au | DMPS | DMPS. . (Au | DMPE | DMPE data from [27], Au | DMPE | DMPE data from [28].)

Turning to the case where DMPE faces Au, the capacity increases in order DMPE < DMPC < DMPS, which seems to follow the expected order of solvent content of the outer layer (therefore, the apparent coverage by lipid is lowest for DMPS). Where DMPE faces the electrolyte, both DMPE and DMPS have high coverage but DMPC has lower coverage. Although we might expect the higher solvent content of DMPS to raise the capacitance, it is possible that the Au-facing layer contains less water because of the drying step essential between the two depositions. DMPS can offset this penalty by interacting directly through hydrogen bonding between headgroups (it contains a hydrogen bond donor and two hydrogen bond acceptors) and the headgroups are tightly packed within the monolayer from which the deposition is made. The electrolyte-facing DMPS may solvate more readily once the electrode is in contact with water again. There is some evidence for a higher solvent content of the outer monolayer of a mixed DMPE/DMPS bilayer from earlier neutron reflectivity results [33] so it is not surprising if the Au-facing layer is relatively solvent-free at low charge densities. Instead, we suggest the differences may arise from a greater mismatch in packing between DMPC with DMPE than between DMPS and DMPE, given previous IR results for chain tilt angle [7,26–29]. Consequently, more defects may form within the DMPC monolayer.

When DMPS faces Au, the results for DMPS and DMPC facing the solution are similar, whereas when DMPE faces the solution, lower capacities are observed, similarly to the case for Au | DMPC | DMPE. DMPE may be forming a barrier to solvent penetration. Lastly, when DMPS faces the electrolyte, highest capacities are seen for the Au | DMPS | DMPS film, with DMPE and DMPC giving similar capacity at -0.2 V and -0.1 V. At 0.2 V, the DMPC capacity starts to rise, as before. The inter-relationships are evidently rather complex and it is difficult to state whether one layer dominates the phase behaviour. Nevertheless, two main points can be made from comparisons of the differential capacity plots: inclusion of DMPS always increases capacity (probably because the molecules are more strongly solvated [28]) and DMPE always reduces capacity (probably because of the strong intermolecular interactions, which tend to lead to exclusion of solvent from the DMPE monolayers [27]). Dynamic effects should also not be excluded, since DMPE and DMPS films are very tightly packed and highly ordered [27,28], whereas DMPC is in the ripple phase [4, 32,33] and so tends to be more fluid at these temperatures; the chain melting phase transitions between gel-like phases and liquid crystalline phases occur at temperatures of 24°C for DMPC [44,45], 49–50°C for DMPE [44,46] and 39°C for DMPS [47].

### *3.1 Chronocoulometry measurements*

Chronocoulometry measurements were also performed on the bilayers, to determine their thermodynamically-controlled behaviour and as a prelude to future structural studies, in which lipid layers are studied under equilibrium conditions. Chronocoulometry data comparing the DMPC/DMPE layers are presented in Figure 4a, data for the DMPC/DMPS system are presented in Figure 4b and the results for the DMPE/DMPS systems are presented in Figure 4c. (The error bars represent standard deviations from three independent measurements.) Similar changes in charge density on adsorption and phase transition are observed in each plot and the form of the plots closely resembles previously published results for symmetric bilayers of the three phospholipids [7,27,28]. The molecules are desorbed at negative potentials, where the plots for lipid-coated layers are merged

with that of the base electrolyte. The adsorption process and phase transitions observed in the differential capacitance results are manifested as steps in charge density in the chronocoulometry results. The differences between the different lipid bilayers that are seen in the capacitance data are mirrored, to some extent, in the chronocoulometry plots. The biggest differences are seen for the DMPE/DMPS systems. In this case, the charge density of the Au | DMPS | DMPE bilayer is always less negative than that of the Au | DMPE | DMPS bilayer. The curve for the mixed bilayer, with 1:1 DMPE and DMPS in each monolayer, is very similar to that obtained for the Au | DMPE | DMPS bilayer. The differences in charge density between the two asymmetric bilayers lie outside of the error bars for each point. It should be noted that the chronocoulometry experiment involves monitoring the charge as the molecules are desorbed, after which the molecules are allowed to re-adsorb. Hence, it should be taken into account that lipid molecules could re-adsorb with a different distribution across the bilayer (*i.e.* the asymmetry might not be maintained upon re-adsorption). In this case, we would expect that a mixing of the molecules would cause the curves to merge together as molecules became jumbled. The fact that corresponding points on the two curves remain separate throughout the potential range suggests that mixing does not take place between DMPE and DMPS. This is to be expected, given the relatively tight packing of the molecules. A shift in the pzc is observed for bilayer-coated electrodes, which is related to an asymmetry in the charge distribution across the bilayer, which causes a small dipole moment across the bilayer [7, 26]. For neutral molecules, the shift in the pzc ( $E_N$ ) is given by Eqn. 2 [7, 48]:

$$E_N = \Gamma(\mu^{\text{org}} - n\mu^{\text{w}})/\epsilon \quad \text{Eqn. 2}$$

where  $\Gamma$  is the surface concentration of molecules,  $\mu^{\text{org}}$  and  $\mu^{\text{w}}$  are the normal components of the dipoles arising from organic molecules and from water, respectively,  $n$  is the number of water molecules displaced per organic molecule and  $\epsilon$  is the permittivity. Although DMPS is an anionic molecule, the small values of the shift in pzc suggest that the molecules adsorb on Au with counterions and/or that their charges are well screened [28]. Certainly the shift is smaller than previously measured for anionic molecules [49]. Here we treat  $\mu^{\text{org}}$  as an overall dipole moment arising from asymmetry in charge distribution across the bilayer, which could equally arise from different surface dipole orientations in each half.  $\mu^{\text{w}}$  is expected to be small and negative [7, 48]; the more negative the shift, the more negative the  $\mu^{\text{org}}$  term for a given surface concentration. In the case of DMPE and DMPS, the surface concentrations are similar because the films were deposited at similar area per molecule, so differences in  $E_N$  arise mainly from differences in the degree of asymmetry in headgroup dipole moment across the bilayer. This might result from a buried negative charge in the Au-facing layer for Au | DMPS | DMPE or it could mean that the dipoles of the headgroups are oriented differently on each side of the bilayer. Moncelli *et al.* suggested that, while PC headgroups could adopt a close to planar conformation, the PS headgroup could as easily be oriented with the phosphate group directed toward the hydrocarbon chain region as oriented with all three charges within the same plane [15]. However, molecular dynamics simulations suggest near-planar (if slightly different) orientations of PC and PE headgroups (in fluid bilayers), with a P-N vector that has its nitrogen atom directly slightly toward the solution (for PC) [50], whereas PS headgroups were observed to orient with the P-N vector pointing with the nitrogen atom slightly inward and the carboxylate group closer to the solution [51,52]. Hydrogen bonding in PS occurs predominantly between ammonium and phosphate groups, as for PE layers, and sodium counterions

are associated primarily with carboxylate groups, thereby screening charges and so allowing close-packing of headgroups [52]. In either case, it is possible that the headgroup orientation of DMPS on Au is different from that facing the electrolyte. When mixed with DMPE within a monolayer, the orientation of the PS headgroup may be altered by hydrogen bonding interactions with the DMPE, which will in turn influence dipole orientation in the Au-facing layer, potentially resulting in similarity for the Au|DMPE|DMPS and DMPE+DMPS films. There may also be similarity in charge distribution in a 50% and 100% DMPS water-facing layer if the two layers do not differ in orientation. Becucci *et al.* [16] also pointed out that the surface dipole of a supported monolayer contains a contribution from orientation of water dipoles associated with the headgroups, which is different for neutral and anionic lipids (in addition to a dipole likely to be associated with the ester groups common to all phosphoglycerolipids). The electrolyte-facing DMPS and the electrode-facing DMPS will have different accessibility to water and so the water contribution to the surface dipole will be different for the two cases.

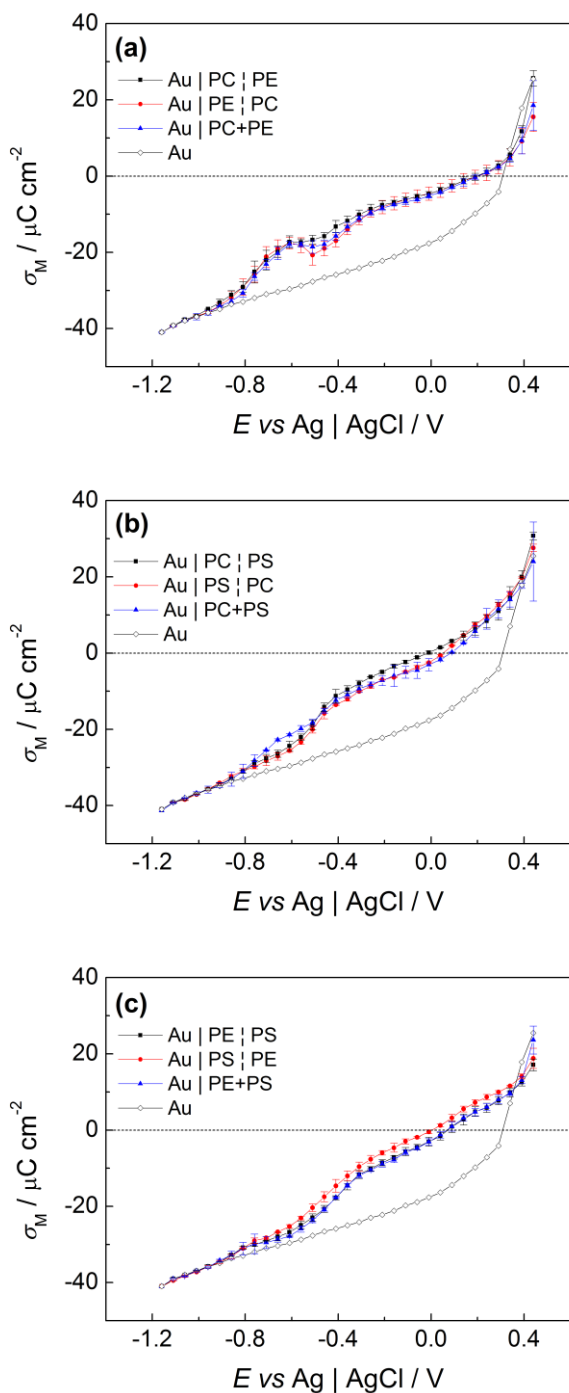


**Figure 4** Charge density vs potential plots for bilayers of different compositions, measured in 0.1 M NaF. Open shapes 0.1 NaF. (a) ■ Au | DMPC | DMPE, ● Au | DMPE | DMPC, ▲ Au | PC+PE. (b) ■ Au | DMPC | DMPS, ● Au | DMPS | DMPC, ▲ Au | PC+PS. (c) ■ Au | DMPE | DMPS, ● Au | DMPS | DMPE, ▲ Au | PS+PE.

The data for the DMPC/DMPS systems show that Au | DMPC | DMPS bilayers have less negative charge density than the Au | DMPS | DMPC bilayers, the opposite trend to DMPE/DMPS layers, and the mixed bilayer curve closely follows the Au | DMPS | DMPC curve. The difference in trend is

unexpected; given that each bilayer contains a zwitterionic molecule and an anionic molecule, one might expect charge asymmetry across a bilayer to be similar for DMPC/DMPS and for DMPE/DMPS. The density of DMPC molecules on the surface is different from those of DMPE and DMPS ( $3.69 \times 10^{-10} \text{ mol cm}^{-2}$  vs  $4.75 \times 10^{-10} \text{ mol cm}^{-2}$  and  $4.55 \times 10^{-10} \text{ mol cm}^{-2}$ ), which would affect the magnitude of any dipole moment arising from the DMPC headgroup or carbonyl orientation relative to DMPS. It is also possible that the greater fluidity of the Au-facing DMPC layer disrupts packing in the DMPS layer, permitting more flexibility for the headgroups of the electrolyte-facing DMPS layer to adopt a different conformation and orientation, which may affect its headgroup solvation and hence surface dipole. The relationship between DMPC and DMPS monolayers may also be complicated by the fact that they exhibit different changes in structure as the potential is varied. When the molecules are adsorbed on the Au surface, DMPC hydrocarbon chains are more tilted than DMPS chains (which have similar tilt angle to those of DMPE). As the potential is made more negative and water forms a cushion between the Au and the bilayer, DMPC chains become less tilted but DMPS chains become much more tilted. Whether these changes are dominated by the response of the Au-facing layer or electrolyte-facing layer is not clear but the opposing trends may be a factor in the overall response of an asymmetric bilayer to an applied electric field.

There is virtually no difference between the chronocoulometry results obtained for the three DMPC/DMPE bilayers, aside from small variations in shape around the adsorption step. This result could indicate that the two asymmetric bilayers simply have identical behaviour or it could mean that the molecules mix on desorption and re-adsorption. The latter seems unlikely in the light of the other results for DMPC/DMPS and DMPE/DMPS bilayers but, to determine whether or not mixing occurs, each measurement was repeated with a fresh bilayer for each data point. These data are presented in Figure 5 and are within an acceptable error margin. From these results we conclude that the differences in differential capacity curves may reflect subtle differences in dynamic behaviour of the bilayers because these measurements are made with an, albeit small, potential sweep, whereas the chronocoulometry data normally reflect equilibrium behaviour. The fact that the chronocoulometric results are so close suggests that headgroups may be adopting similar conformations in each case and that these are similar in turn to those observed for symmetric bilayers of each molecule.

We assume that mixing does not take place while the molecules are adsorbed and that the bilayers are in a highly metastable state. DMPC and DMPE have been reported to have moderate, although limited, miscibility and ideal mixing is not observed [53–55], probably because of the difference in nature of inter-headgroup interactions between PE and PC molecules (*i.e.* PE-PE  $\neq$  PE-PC  $\neq$  PC-PC). The miscibility indicates there is an overall thermodynamic driving force for mixing. For mixing to occur between the molecules in an initially asymmetric bilayer, an activation energy must be overcome for molecules to translocate (“flip-flop”) between the two halves of the bilayer. Such activation energies have been measured by Conboy and co-workers, using sum-frequency vibrational spectroscopy (SFVS) with bilayers containing one deuterated component [38–41]. The measurements indicate relatively fast flip-flop for PC-based bilayers but the measurements differ from ours in that they were made on silica substrates (presumably with some adsorbed water) and were carried out (mostly) at LB-LS deposition pressures of  $30 \text{ mN m}^{-1}$ , which is a more fluid, less close-packed phase than in our measurements. We may thus expect higher activation energies for flip-flop in our bilayers. Anglin and Conboy found that distearoyl phosphatidylethanolamine (DSPE) traverses the

membrane at a rate two orders of magnitude slower than distearoyl phosphatidylcholine (DSPC) at a given pressure and related this effect to differences in packing and solvation between the two types of headgroup [40]. In our case, DMPE was deposited at a higher packing density and surface pressure, in the solid phase, and so the activation barrier should be considerably higher in our bilayers than in the SFVS experiments. It is also possible that interaction with the gold substrate may slow the rate of translocation. Similar arguments apply for DMPC/DMPS systems. DMPC and DMPS mix, although mixing is far from ideal [56,57]. The phase behaviour deviates strongly from that predicted for a phase diagram of an ideal mixture of the two components [56] and excess areas are observed in Langmuir isotherm measurements [57]. There does not appear to be a strong consensus as to whether PS is randomly dispersed in PC or forming small clusters. Coulombic repulsion between headgroups appears to be offset by interactions with sodium counterions and direct hydrogen bonding is possible between PS headgroups. These factors may result in the non-ideal mixing behaviour observed. Flip-flop, as measured with SFVS, of PS across a silica|PC|PC-PS bilayer is slower than for PC and depends strongly on the PS mole fraction (slowing for higher mole fractions) [41]. Again, these studies were carried out at lower deposition surface pressures than for our bilayers and this, combined with the point that we initially start with a 100% DMPS monolayer, suggest that flip-flop should also be relatively slow for the DMPC/DMPS asymmetric bilayers. DMPE and DMPS do mix ideally [58], which might be expected from the similarity in size, shape and nature of interactions of these two headgroups. Consequently we might expect the strongest driving force for mixing in our DMPE/DMPS bilayers, yet in this case the activation barrier is highest because of the tight packing present in each half of the bilayer. Some evidence to support the conclusion that asymmetry is maintained in our systems may be found in previous PM-IRRAS results for Au | DMPC | DMPC [26] and Au | DMPE | DMPE systems [29], in which selective deuteration was employed to study one monolayer at a time. Different tilt angles were measured for the Au-facing monolayer and solution-facing monolayer in each case. Had the molecules mixed, the same chain tilt angles would have been observed for the two halves of the bilayer (an average over the two halves).

We surmise, therefore, that the similarity in chronocoulometry results for Au|DMPC|DMPE and Au|DMPE|DMPC arise from comparable headgroup orientations (likely close to parallel) in the two cases and that more difference is observed for DMPC/DMPS and DMPE/DMPS bilayers because of different dipole orientation and solvation in DMPS monolayers, as suggested by molecular dynamics simulations [51,52]. The interaction of the carboxylate moiety of the serine group with sodium and/or water and possible different orientation of water dipoles around carbonyl groups [16] (which might also interact with ammonium groups) may also influence charge distribution at the DMPS|water interface and so result in differences in measured charge density between bilayers where DMPS is deposited first or second.



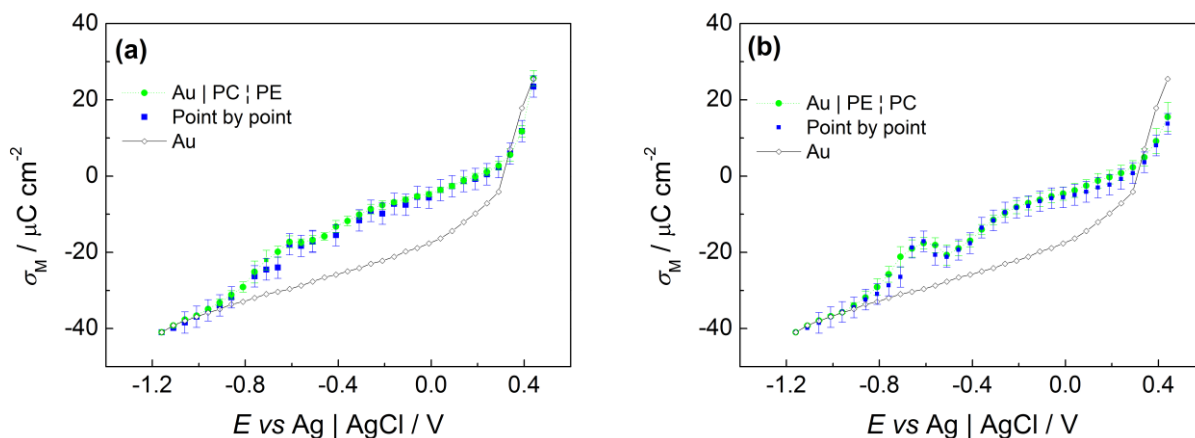


**Figure 5** Charge density vs potential plots for asymmetric DMPC/DMPE bilayers where each point was measured for a fresh bilayer. Open shapes bare Au in 0.1 M NaF. (a) ● Au | DMPC | DMPE from Figure 4, ■ Au | DMPC | DMPE point by point. (b) ● Au | DMPE | DMPC from Figure 4, ■ Au | DMPE | DMPC point by point. Error bars on the data from Figure 4 represent the standard deviation from three bilayer measurements. The largest error bar in each case was used to provide the error bars for the point by point data.

As with the differential capacitance data, it is helpful to compare plots where the gold-facing monolayers are the same and to compare plots where the electrolyte-facing monolayers are the same. These comparisons are made in Figure 6. It is interesting to see that when DMPS is the LB layer on the gold, there is very little difference in electrochemical behaviour between the bilayers. Apparently the structure of this DMPS layer determines overall bilayer properties. In contrast, when DMPS faces the solution, different charge densities are obtained for the three bilayers: the phase transition is shifted to more negative potentials for DMPC and DMPS and the charge densities are less negative for these molecules. These differences probably result from differences in headgroup (and hence dipole) orientation of the gold-facing layers, although if the outer layer's packing is affected by the bottom layer, the accessibility of the DMPS headgroups to water will be affected. In any case, it seems likely that the DMPS molecules are organised differently when deposited on different monolayers.

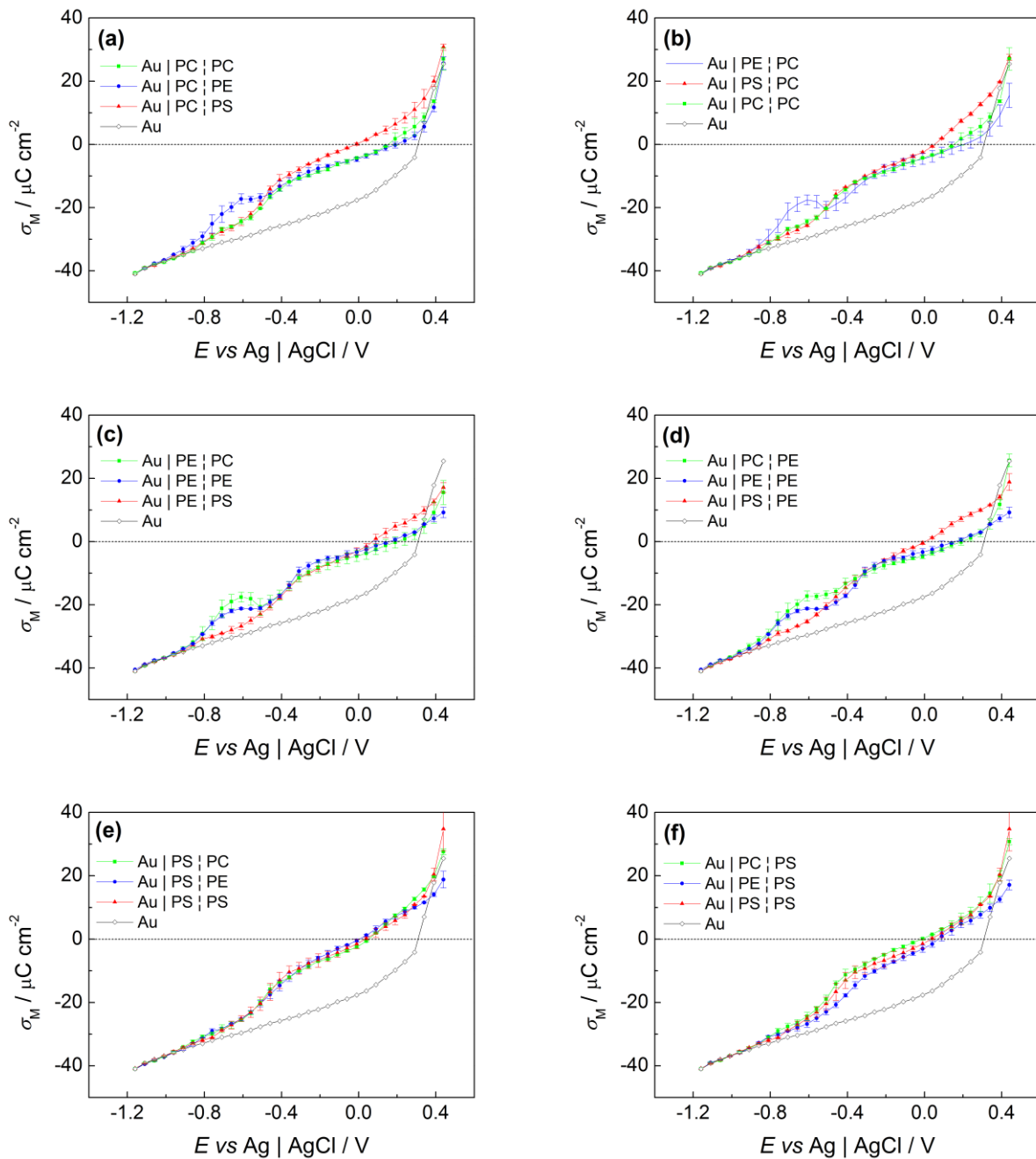


**Figure 6** Charge density vs potential plots comparing bilayers with a common layer. Open shapes bare Au in 0.1 M NaF. (a) ■ Au | DMPC | DMPC, ● Au | DMPC | DMPE, ▲ Au | DMPC | DMPS. (b) ■ Au | DMPC | DMPC, ● Au | DMPE | DMPC, ▲ Au | DMPS | DMPC. (c) ■ Au | DMPE | DMPC, ● Au | DMPE | DMPE, ▲ Au | DMPE | DMPS. (d) ■ Au | DMPC | DMPE, ● Au | DMPE | DMPE, ▲ Au | DMPS | DMPE. (e) ■ Au | DMPS | DMPC, ● Au | DMPS | DMPE, ▲ Au | DMPS | DMPS. (f) ■ Au | DMPC | DMPS, ● Au | DMPE | DMPS, ▲ Au | DMPS | DMPS. (Au | DMPE | DMPE data from [27], Au | DMPE | DMPE data from [28].)

Comparing the bilayers where DMPE faces the electrode, similar results are obtained for DMPE and DMPC facing solution, whereas DMPS charge density plots are much more sloped and the adsorption step is less pronounced. The same is observed for the bilayers where DMPE faces the electrolyte. The higher slope is a reflection of the higher capacitance of these DMPS-containing bilayers. For bilayers which have DMPC in common, again, the DMPS-containing bilayers tend to have higher slope (and therefore capacitance) than the bilayers containing neutral molecules. Some small differences are observed between DMPC and DMPE at more positive potentials, in the region where charge density on the metal is low. In each case, the presence of DMPE results in lower capacitance. The adsorption step of DMPE-containing bilayers is also more pronounced.

In summary, it is apparent that the presence of DMPS in a bilayer has the strongest effect on charge density, which is likely to be a result of its being strongly solvated. Differences in charge distribution across the bilayers are observed when DMPS is combined with DMPE or DMPC. Bilayers composed of DMPE and DMPC give practically the same charge density, which suggests that the orientation of zwitterionic headgroups is likely to be similar in each case. PM-IRRAS studies of symmetric DMPC and DMPE bilayers showed similar orientation of the phosphate groups when the molecules were directly adsorbed on the Au, although it should be borne in mind that the spectra are an average of both halves of the bilayer. DMPE monolayers seem to retain the behaviour observed in symmetric systems and tend to resist solvent ingress, which indicates that their tight packing is difficult to disturb. However, the fact that some distinct electrochemical responses are seen suggests that different monolayer structures (*e.g.* orientation, fluidity or solvent content) may affect one another in a complex way and highlights the importance of asymmetry in designing supported bilayers. Future structural studies will shed light on these relationships: our preliminary IR data suggest that chain orientation can differ between symmetric and chemically asymmetric bilayers.

#### **4. Conclusions**

Differential capacity and chronocoulometry measurements have been used to study chemically asymmetric phospholipid bilayers supported on Au(111) electrodes. We show that the bilayers retain their asymmetry over the timescale of the experiments and that the relative location of the two phospholipids has an impact on the measured capacitance of the bilayer and charge density-potential plot. When DMPE forms part of the bilayer, its tight packing and low solvent content tend to cause a reduction in the capacitance of the bilayer. DMPS, on the other hand, is more strongly solvated and this incorporation of solvent into DMPS-containing bilayers leads to higher capacitance, which is observed in both differential capacitance and charge density-potential plots. When asymmetric films are formed from DMPE and DMPC, the equilibrium behaviour is indistinguishable but subtle differences in differential capacitance measurements can be observed. The main significance of our findings is that it is possible to study asymmetric layers, which is a step toward more biologically relevant models of cell membranes. The relative location of a charged lipid within a bilayer influences electrochemical properties and therefore careful design of model bilayers is needed for studies where the rôle of charged lipids in a membrane is explored, for example in studies of specific lipid-protein interactions.

#### **5. Acknowledgements**

E.M. acknowledges the School of Chemistry, University of Birmingham, for a studentship.

## References

- [1] B. Alberts, A. Johnson, J. Lewis, M. Raff, K. Roberts, P. Walter, *Molecular Biology of the Cell*, 4th Ed., Taylor and Francis, 2002, Ch 10.
- [2] M. Cheever, M. Overduin, in *Modular Protein Domains* Ed. Cesareni, Wiley 2004.
- [3] M. Overduin, M. M.L. Cheever, T.G. Kutateladze, Signalling with phosphoinositides: better than binary, *Molec. Interv.*, 8 (2001) 1, 150–159.
- [4] J. Lipkowski, Building biomimetic membrane at a gold electrode surface, *Phys. Chem. Chem. Phys* 12 (2010) 13874–13887.
- [5] S.L. Horswell, V. Zamlynny, H-Q. Li, A.R. Merrill, J. Lipkowski, Electrochemical and PM-IRRAS studies of potential controlled transformations of phospholipid layers on Au(111) electrodes, *Faraday. Discuss.* 121 (2002) 405–422.
- [6] I. Burgess, M. Li, S.L. Horswell, G. Szymanski, J. Lipkowski, J. Majewski, S. Satija, Electric field-driven transformations of a supported model biological membrane – An electrochemical and neutron reflectivity study, *Biophys. J.* 86 (2004) 1763–1776.
- [7] I. Zawisza, X. Bin, J. Lipkowski, Potential-driven structural changes in Langmuir-Blodgett DMPC bilayers determined by in situ spectroelectrochemical PM IRRAS, *Langmuir* 23 (2007) 5180–5194.
- [8] R. Guidelli, G. Aloisi, L. Becucci, A. Dolfi, M.R. Moncelli, F.T. Buoninsegni, Bioelectrochemistry at metal | water interfaces, *J. Electroanal. Chem.* 504 (2001) 1–28.
- [9] D. Bizzotto, A. Nelson, Continuing electrochemical studies of phospholipid monolayers of dioleoyl phosphatidylcholine at the mercury–electrolyte interface, *Langmuir* 14 (1998) 6269–6273.
- [10] A. Nelson, F.A.M. Leermakers, Substrate-induced structural changes in electrode-adsorbed lipid layers: Experimental evidence from the behaviour of phospholipid layers on the mercury–water interface, *J. Electroanal. Chem.* 278 (1990) 73–83.
- [11] C. Whitehouse, R. O’Flanagan, B. Lindholm-Sethson, B. Movaghar, A. Nelson, Application of electrochemical impedance spectroscopy to the study of dioleoyl phosphatidylcholine monolayers on mercury, *Langmuir* 20 (2004) 136–144.
- [12] A. Nelson, Electrochemistry of mercury supported phospholipid monolayers and bilayers, *Curr. Opin. Coll. Interf. Sci.* 15 (2010) 1455–1466.
- [13] M. Rueda, I. Navarro, F. Prieto, A. Nelson, Impedance measurements with phospholipid-coated mercury electrodes, *J. Electroanal. Chem.* 454 (1998) 155–160.

- [14] M. Rueda, F. Prieto, I. Navarro, R. Romero, Phospholipid and gramicidin- phospholipid-coated mercury electrodes as model systems of partially blocked electrodes, *J. Electroanal. Chem.* 649 (2010) 42–47.
- [15] M.R. Moncelli, L. Becucci, F.T. Buoninsegni, R. Guidelli, Surface dipole potential at the interface between water and self-assembled monolayers of phosphatidylserine and phosphatidic acid, *Biophys. J.* 74 (1998) 2388–2397.
- [16] L. Becucci, M.R. Moncelli, R. Herrero, R. Guidelli, Dipole potentials of monolayers of phosphatidylcholine, phosphatidylserine and phosphatidic acid on mercury, *Langmuir* 16 (2000) 7694–7700.
- [17] F.T. Buoninsegni, L. Becucci, M.R. Moncelli, R. Guidelli, Total and free charge densities on mercury coated with self-assembled phosphatidylcholine and octadecanethiol monolayers and octadecanethiol phosphatidyl choline bilayers, *J. Electroanal. Chem.* 500 (2001) 395–407.
- [18] M.R. Moncelli, L. Becucci, A. Nelson, R. Guidelli, Electrochemical modeling of electron and proton transfer to ubiquinone-10 in a self-assembled phospholipid monolayer, *Biophys. J.* 70 (1996) 2716–2726.
- [19] G.J. Gordillo, D.J. Schiffrin, The electrochemistry of ubiquinone-10 in a phospholipid model membrane, *Faraday Disc.* 116 (2000) 89–107.
- [20] A. Nelson, Effect of lipid charge and solution composition on the permeability of phospholipid–gramicidin monolayers to  $\text{Ti}^+$ , *J. Chem. Soc. Faraday Trans.* 15 (1993) 2799–2805.
- [21] M. Rueda, I. Navarro, G. Ramirez, F. Prieto, C. Prado, A. Nelson, Electrochemical impedance study of  $\text{Ti}^+$  reduction through gramicidin channels in self-assembled gramicidin-modified dioleoylphosphatidylcholine monolayers on mercury electrodes, *Langmuir* 15 (1999) 3672–3678.
- [22] M. Rueda, I. Navarro, C. Prado, C. Silva, Impedance study of  $\text{Ti}^+$  reduction at gramicidin-modified dioleoylphosphatidylcholine-coated mercury electrodes: influence of gramicidin concentration and the nature of the supporting electrolyte, *J. Electrochem. Soc.* 148 (2001) E139–E147.
- [23] L. Becucci, V. Tramonti, A. Fiore, V. Fogliano, A. Scaloni, R. Guidelli, Channel-forming activity of syringomycin E in two mercury-supported biomimetic membranes, *Langmuir* 31 (2015), 932–941.
- [24] L. Becucci, R. Guidelli, Can gramicidin ion channel affect the dipole potential of neighboring phospholipid headgroups? *Bioelectrochem.* 106 (2015), 343–352.
- [25] A. Nelson, Electrochemistry of mercury supported phospholipid monolayers and bilayers, *Curr. Opin. Coll. Interf. Sci.* 15 (2010) 455–466.
- [26] N. Garcia-Araez, C.L. Brosseau, P. Rodriguez, J. Lipkowski, Layer by layer PMIRRAS characterization of DMPC bilayers deposited on a Au(111) electrode surface, *Langmuir* 22 (2006), 10365–10371.

- [27] E. Madrid, S.L. Horswell, Effect of headgroup on the physicochemical properties of phospholipid bilayers in electric fields: size matters, *Langmuir* 29 (2013) 1695–1708.
- [28] E. Madrid, S.L. Horswell, Effect of electric field on structure and dynamics of bilayers formed from anionic phospholipids, *Electrochim. Acta* 146 (2014), 850–860.
- [29] E. Madrid, S.L. Horswell, Effect of deuteration on the phase behaviour of supported phospholipid bilayers: a spectroelectrochemical study, *Langmuir* 31 (2015), 12544–12551.
- [30] J.J. Leitch, C.L. Brosseau, S.G. Roscoe, K. Bessonov, J.R. Dutcher, J. Lipkowski, Electrochemical and PM-IRRAS Characterization of Cholera Toxin Binding at a Model Biological Membrane, *Langmuir*, 29 (2013), 965-976.
- [31] M. Chen, M. Li, C.L. Brosseau, J. Lipkowski, AFM studies of the effect of temperature and electric field on the structure of a DMPC-cholesterol bilayer supported on an Au(111) electrode surface, *Langmuir* 25 (2009) 1028–1037.
- [32] S. Xu, G. Szymanski, J. Lipkowski, Self-assembly of phospholipid molecules at a Au(111) electrode surface, *J. Am. Chem. Soc.* 126 (2004) 12276–12277.
- [33] A.R. Hillman, K.S. Ryder, E. Madrid, A.W. Burley, R.J. Wiltshire, J. Merotra, M. Grau, S.L. Horswell, A. Glidle, R.M. Dalgliesh, A. Hughes, R. Cubitt, A. Wildes, Structure and dynamics of phospholipid bilayer films under electrochemical control, *Faraday Discuss.* 145 (2010) 357–379.
- [34] S. Sek, T. Laredo, J.R. Dutcher, J. Lipkowski, Molecular resolution imaging of an antibiotic peptide in a lipid matrix, *J. Am. Chem. Soc.* 131 (2009) 6439–6444.
- [35] M. Smetanin, S. Sek, F. Maran, J. Lipkowski, Molecular resolution visualization of a pore formed by trichogin, an antimicrobial peptide, in a phospholipid matrix, *Biochim. Biophys. Acta - Biomembranes*, 1838 (2014), 3130–3136.
- [36] P. Pieta, M. Majewska, Z.F. Su, M. Grossutti, B. Wladyka, M. Piejko, J. Lipkowski, P. Mak, Physicochemical studies on orientation and conformation of a new bacteriocin BacSp222 in a planar phospholipid bilayer, *Langmuir*, 23 (2016), 5653–5662.
- [37] ZF Su, J.J. Leitch, R.J. Faragher, A.L. Schwan, J. Lipkowski, Gramicidin A ion channel formation in model phospholipid bilayers tethered to gold (111) electrode surfaces, *Electrochim. Acta*, 243 (2017), 364–373.
- [38] J. Liu, J.C. Conboy, Direct measurement of the transbilayer movement of phospholipids by sum-frequency vibrational spectroscopy, *J. Am. Chem. Soc.* 126 (2004) 8376–8377.
- [39] J. Liu, J.C. Conboy, 1,2-diacyl-phosphatidylcholine flip-flop measured directly by sum-frequency vibrational spectroscopy, *Biophys. J.* 89 (2005) 2522–2532.

- [40] T.C. Anglin and J. C. Conboy, Kinetics and thermodynamics of flip-flop in binary phospholipid membranes measured by Sum-Frequency Vibrational Spectroscopy, *Biochemistry*, 48 (2009), 102202–10234.
- [41] K.L. Brown, J.C. Conboy, Lipid flip-flop in binary membranes composed of phosphatidylserine and phosphatidylcholine, *J. Phys. Chem. B*, 117 (2013), 15041–15050.
- [42] J. Richer, J. Lipkowski, Measurement of physical adsorption of neutral organic species at solid electrodes, *J. Electrochem. Soc.* 133 (1986) 121–128.
- [43] B.B. Damaskin, O.A. Petrii, V.V. Batrakov, Adsorption of organic compounds on electrodes, Nauka, Moscow, 1968.
- [44] H. Casal, H.H. Mantsch, Polymorphic phase behaviour of phospholipid membranes studied by infrared spectroscopy, *Biochim. Biophys. Acta* 770 (1984), 381–401.
- [45] C.H. Chen, Interactions of lipid vesicles with solvent in heavy and light water, *J. Chem. Phys.* 77 (1982), 4408–4416.
- [46] R.N.A.H. Lewis, R.N. McElhaney, Calorimetric and spectroscopic studies of the polymorphic phase behaviour of a homologous series of n-saturated 1,2-diacyl phosphatidylethanolamines, *Biophys. J.* 64 (1993), 1081–1096.
- [47] H.L. Casal, H.H. Mantsch, Infrared studies of fully hydrated saturated phosphatidylserine bilayers. Effect of  $\text{Li}^+$  and  $\text{Ca}^{2+}$ , *Biochemistry* 26 (1987) 4408–4416.
- [48] J. Lipkowski, L. Stolberg, in Adsorption of molecules at metal electrodes, J., Lipkowski, P. N. Ross, (Eds.) VCH, New York, 1992, pp. 171–238.
- [49] I. Burgess, V. Zamlynny, G. Szymanski, J. Lipkowski, J. Majewski, G. Smith, S. Satija, R. Ivkov, Electrochemical and neutron reflectivity characterization of dodecyl sulfate adsorption and aggregation at the gold–water interface, *Langmuir* 17 (2001) 3355–3367.
- [50] A.A. Gurtovenko, I. Vattulainen, Lipid transmembrane asymmetry and intrinsic membrane potential: two sides of the same coin, *J. Am. Chem. Soc.* 129 (2007), 5358–5359.
- [51] S.A. Pandit and M.L. Berkowitz, Molecular dynamics simulation of dipalmitoylphosphatidylserine bilayer with  $\text{Na}^+$  counterions, *Biophys. J.* 82 (2002), 1818–1827.
- [52] S.A. Pandit, D. Bostick, M.L. Berkowitz, Mixed bilayer containing dipalmitoylphosphatidylcholine and dipalmitoylphosphatidylserine: lipid complexation, ion binding, and electrostatics, *Biophys. J.* 85 (85 (2003), 3120–3131.
- [53] I.P. Sugár, G. Monticelli, Interrelationships between the phase diagrams of the two-component phospholipid bilayers, *Biophys. J.* 48 (1985), 283–288.
- [54] J.R. Silvius, Solid- and liquid-phase equilibria in phosphatidylcholine / phosphatidylethanolamine mixtures. A calorimetric study. *Biochim. Biophys. Acta*, 857 (1986), 217–228.

- [55] I.V. Polozov, J.G. Molotkovsky, L.D. Bergelson, Anthrylvinyl-labeled phospholipids as membrane probes: the phosphatidylcholine-phosphatidylethanolamine system, *Chem. Phys. Lipids*, 69 (1994), 209–218.
- [56] J.R. Silvius, J. Gagné, Calcium-induced fusion and lateral phase separations in phosphatidylcholine-phosphatidylserine vesicles. Correlation by calorimetric and fusion measurements. *Biochemistry*, 23 (1984), 3241–3247.
- [57] C. Luna, K.M. Stroka, H. Bermudez, H. Aranda-Espinoza, Thermodynamics of monolayers formed by mixtures of phosphatidylcholine/phosphatidylserine, *Coll. Surf. B*, 85 (2011), 293–300.
- [58] J.R. Silvius, J. Gagné, Lipid phase behavior and calcium-induced fusion of phosphatidylethanolamine–phosphatidylserine vesicles. Calorimetric and fusion studies. *Biochemistry*, 23 (1984), 3232–3240.